myocardial bundles were disturbed and edematous. Edema with infiltration by small lymphocytes and macrophages was observed between the myocardial bundles. E. Immunohistochemical analysis of CD8. F. Small granulomas with giant cells were found in the myocardium.

blood. Blood culture was conducted at the time of autopsy and demonstrated no significant bacterial growth. A chest radiograph showed abnormal infiltration in the right hilar area and lower lung field, and an increased cardiothoracic ratio. The lateral view also showed a posteriorly displaced major bronchus.

The patient was administered oxygen and inhaled salbutamol in the emergency room. Her respiratory rate and mode of respiration improved after inhalation, and she was diagnosed with a severe asthmatic attack complicated with a suspected lower respiratory infection and admitted to a pediatric ward. Three hours after admission, her respiratory condition deteriorated. Transfer to the intensive-care unit was determined and additional examinations and intubation was performed. A blood test revealed an extremely high brain natriuretic peptide level (6,788 pg/ml), whereas her creatine phosphokinase, lactate dehydrogenase, and aspartate aminotransferase levels were in the normal ranges. An echocardiogram was unremarkable, but an electrocardiogram was not performed. Cardiac arrest occurred suddenly after intubation. Resuscitation efforts were unsuccessful and the patient died 8 hour after admission. A morbid autopsy was performed within 6 hours of death. Macroscopically, the patient's heart was large and the left ventricle was dilated. There was no thrombus in the lumen or significant change in the four valves. Severe diffuse infiltration of small lymphocytes and macrophages was observed histologically in the myocardium (**Figure 1**). Immunohistochemistry showed that a large proportion of the small lymphocytes were $CD8^+$ T cells. Small granulomas with giant cells were found in the myocardium. There was no necrosis, and no disturbance of the myocardial array was observed. Small granulomas were also found in the lung and liver. Neither fungi nor acid-fast bacilli were found. In the both lungs, diffuse and mild lymphoplasmacytic infiltration of the bronchial and alveolar wall was observed.

Materials and methods

To identify any pathogen causing myocarditis, DNA and RNA samples extracted from a frozen sample of the heart were analyzed with a multi-virus real-time PCR system, which can examine 163 viruses simultaneously on a 96-well plate [3]. Although a low copy number of parvovirus B19 (36.1 copies per 100 ng of DNA) was detected in the bronchus, no viral genome was detected in the heart sample with this system. We then analyzed DNA and RNA samples extracted from frozen tissue from the heart with deep sequencing, using a next-generation sequencer (GAIIx, Illumina, San Diego, CA). RNA was reverse transcribed to cDNA, and both DNA and cDNA were applied to the GAIIx. In total, 3×10^7 reads were obtained with the GAIIx, and a BLAST search revealed that 244,965 80-bp reads were nonhuman sequences.

Results

Two of the reads corresponded to nucleotides (nt) 4,535-4,614 and nt 5,034-5,113 of the TSV genome (GU989205). No other significant pathogenic genome was identified. A real-time PCR analysis was performed to detect the TSV VP1 gene using the TSPyV-F primer (5'-cagtgctaatgacaaattggttgttc-3'), TSPyV-R primer (5'-ttagcttttgtttgtagtgaggattga-3'), and TSPyV-FAM probe (5'-FAM-cccaataaaacaccagagcacacaaggc-TAMRA-3'), targeting nt 1,841-1,923 of GU989205. The real-time PCR analysis detected the TSV genome in the heart (413.2 copies per 100 ng of DNA), lung (248.8), liver (81.6), spleen (103.7), bronchus (36.5), small intestine (58.1), and colon (24.1), indicating that the TSV genome copy number was higher in the heart than in the other organs.

Long PCR using KOD-FX DNA polymerase (Toyobo, Tokyo, Japan) amplified the entire TSV genome, with a length of 5,232 bp. We also successfully PCR amplified a 252-bp fragment including a putative replication origin of TSV using two primers (TSV-F5111 5'-agcctctgtgtgcctcaatt-3', and TSV-R131 5'-tcctcaggataacggtcttaa-3') suggesting the presence of a circular form of the TSV genome in the heart sample. The long PCR product of full-length TSV was cloned into the pCR2.1-blunt vector (Invitrogen, Carlsbad, CA). A sequencing analysis of four clones from independent colonies revealed

that the cloned PCR product was 99.4% homologous to the complete genome of previously reported TSV (GU989205 and JQ723730). Therefore, we designated the TSV clone strain TSV-TMC, and registered it in GenBank under accession number AB873001.

Discussion

Polyomaviruses are ~45 nm, nonenveloped, double-stranded DNA viruses with a small genome of ~5.2 kb. Until now, 10 polyomaviruses have been described in humans and the majority of human polyomaviruses (HPyVs) were identified in the last five years [4]. Generally, a primary infection with polyomavirus is thought to be asymptomatic, and the virus persists in immunocompetent individuals as a latent infection during their whole lives. JC polyomavirus and BK polyomavirus are considered to be pathogens that cause progressive multifocal leukoencephalopathy in AIDS patients and nephropathy in renal transplant recipients, respectively. Merkel cell polyomavirus (MCPyV) has been found to be integrated in a large proportion of Merkel cell carcinomas of the skin [5]. HPyV6 and HPyV7 productively infect the human skin, and infections with such skin-tropic polyomaviruses are very common in the general population [6]. A putative association between trichodysplasia spinulosa (TS) and TSV has been considered, but is not definitive [7]. TS is histologically characterized by the abnormal maturation and marked distention of the hair follicles, and is considered to be symptomatic only in immunocompromised patients. However, the actual etiology of TSV has not yet been established.

TSV was detected in the myocardial tissues of a seven-month-old girl with severe myocarditis. This report is notable for two points: (1) TSV was identified in a child who had no remarkable past history and would be immunocompetent; and (2) TSV was detected in tissues other than the skin. Although the seroprevalence of TSV in the general Japanese population is unknown, a high prevalence is predicted in Japan based on the seroprevalence data from European countries [8-11]. It has also been demonstrated that primary TSV infections frequently occur in early life, within 0-10 years after birth [8]. However, no report has described an association between primary TSV infection and any disease. We were unable to determine whether this was a primary infection, but the high copy number of the TSV genome and the presence of the circular form of TSV in the heart suggest a possible role of TSV as a causative agent of myocarditis in some infant cases. Although the molecular mechanism of TSV infection is unknown, this case serves a hypothesis of the presence of specific receptor for TSV in myocytes. Alternatively, TSV might be reactivated and produced in specific organs under the condition of severe inflammation. Histological changes in this case such as severe infiltration of lymphocytes and destruction of myocytes are observed commonly among other viral myocarditis like Coxsackievirus and enterovirus, not specific for TSV. It cannot be completely denied that such severe inflammation induced production of TSV which existed as a bystander there. To determine the association between myocarditis and TSV infection, serological studies and the immunohistochemical detection of the viral proteins in myocarditis samples will be required. Immunohistochemistry and in situ hybridization may be useful for detection of the virus protein or genome in tissue samples, but have not been established, yet, because there is no appropriate control sample or culture cell positive for TSV, so far. The direct relationship between granulomas and TSV infection was considered unlikely, because distribution of the granuloma was not correlated with TSV copy numbers. However, the presence of granulomas implies any immunological abnormality in the patient.

To the best of our knowledge, this is the first case report describing the detection of TSV in a myocarditis specimen from a child. Although we have previously reported that low copy numbers of MCPyV were detected in some tissue samples from myocarditis patients [12], few reports have described the association between polyomavirus infection and myocarditis. Therefore, further studies are required to clarify the association between TSV infection and the pathogenesis of myocarditis.

Acknowledgements

The authors deeply appreciate the sincere cooperation of the parents of the patient. This work was partly supported by Health and Labor Sciences Research Grants (No. H25-Shinko-Ippan 015 to MK and HK) from the Ministry of Health, Labor and Welfare, and a Grant-in-Aid

for Scientific Research from the Ministry of Education, Culture, Sports, Science and Technology of Japan (No. 24659212 to HK).

Disclosure of conflict of interest

None.

Address correspondence to: Dr. Shinya Tsuzuki, Department of Pediatrics, National Center for Global Health and Medicine, 1-21-1 Toyama, Shinjuku-ku, Tokyo 162-0855, Japan. Tel: +81(3)-3202-7181; Fax: +81(3)-3207-1038; E-mail: shinyatsuzuki@yahoo.co.jp

References

[1] Cooper LT Jr. Myocarditis. N Engl J Med 2009; 360: 1526-1538.

[2] van der Meijden E, Janssens RW, Lauber C, Bouwes Bavinck JN, Gorbalenya AE, Feltkamp MC. Discovery of a new human polyomavirus associated with trichodysplasia spinulosa in an immunocompromized patient. PLoS Pathog 2010; 6: e1001024.

[3] Katano H, Kano M, Nakamura T, Kanno T, Asanuma H, Sata T. A novel real-time PCR system for simultaneous detection of human viruses in clinical samples from patients with uncertain diagnoses. J Med Virol 2011; 83: 322-330.

[4] Kazem S, van der Meijden E, Feltkamp MC. The trichodysplasia spinulosa-associated polyomavirus: virological background and clinical implications. APMIS 2013; 121: 770-782.

[5] Feng H, Shuda M, Chang Y, Moore PS. Clonal integration of a polyomavirus in human Merkel cell carcinoma. Science 2008; 319: 1096-1100.

[6] Schowalter RM, Pastrana DV, Pumphrey KA, Moyer AL, Buck CB. Merkel cell polyomavirus and two previously unknown polyomaviruses are chronically shed from human skin. Cell Host Microbe 2010; 7: 509-515.

[7] Kazem S, van der Meijden E, Kooijman S, Rosenberg AS, Hughey LC, Browning JC, Sadler G, Busam K, Pope E, Benoit T, Fleckman P, de Vries E, Eekhof JA, Feltkamp MC. Trichodysplasia spinulosa is characterized by active polyomavirus infection. J Clin Virol 2012; 53: 225-230.

[8] Nicol JT, Robinot R, Carpentier A, Carandina G, Mazzoni E, Tognon M, Touzé A, Coursaget P. Age-specific seroprevalences of Merkel cell polyomavirus, human polyomaviruses 6, 7, and 9, and trichodysplasia spinulosa-associated polyomavirus. Clin Vaccine Immunol 2013; 20: 363-368.

[9] Sadeghi M, Aronen M, Chen T, Jartti L, Jartti T, Ruuskanen O, Söderlund-Venermo M, Hedman K. Merkel cell polyomavirus and trichodysplasia spinulosa-associated polyomavirus DNAs and antibodies in blood among the elderly. BMC Infect Dis 2012; 12: 383.

[10] Chen T, Mattila PS, Jartti T, Ruuskanen O, Soderlund-Venermo M, Hedman K. Seroepidemiology of the newly found trichodysplasia spinulosa-associated polyomavirus. J Infect Dis 2011; 204: 1523-1526.

[11] van der Meijden E, Kazem S, Burgers MM, Janssens R, Bouwes Bavinck JN, de Melker H, Feltkamp MC. Seroprevalence of trichodysplasia spinulosa-associated polyomavirus. Emerg Infect Dis 2011; 17: 1355-1363.

[12] Fukumoto H, Sato Y, Hasegawa H, Katano H. Frequent detection of Merkel cell polyomavirus DNA in sera of HIV-1-positive patients. Virol J 2013; 10: 84.

PLOS ONE

RESEARCH ARTICLE

Complete Genome Sequence and Comparative Genomic Analysis of *Mycobacterium massiliense* JCM 15300 in the *Mycobacterium abscessus* Group Reveal a Conserved Genomic Island MmGI-1 Related to Putative Lipid Metabolism

Tsuyoshi Sekizuka[1*☯], Masanori Kai[2☯], Kazue Nakanaga[2], Noboru Nakata[2], Yuko Kazumi[3], Shinji Maeda[3], Masahiko Makino[2], Yoshihiko Hoshino[2*], Makoto Kuroda[1]

1. Pathogen Genomics Center, National Institute of Infectious Diseases, Tokyo, Japan, **2.** Leprosy Research Center, National Institute of Infectious Diseases, Tokyo, Japan, **3.** Research Institute of Tuberculosis, Japan Anti-Tuberculosis Association, Tokyo, Japan

*sekizuka@niid.go.jp (TS); yhoshino@niid.go.jp (YH)

☯ These authors contributed equally to this work.

OPEN ACCESS

Citation: Sekizuka T, Kai M, Nakanaga K, Nakata N, Kazumi Y, et al. (2014) Complete Genome Sequence and Comparative Genomic Analysis of *Mycobacterium massiliense* JCM 15300 in the *Mycobacterium abscessus* Group Reveal a Conserved Genomic Island MmGI-1 Related to Putative Lipid Metabolism. PLoS ONE 9(12): e114848. doi:10.1371/journal.pone.0114848

Editor: Jean Louis Herrmann, Hopital Raymond Poincare - Universite Versailles St. Quentin, France

Received: February 27, 2014

Accepted: November 14, 2014

Published: December 11, 2014

Funding: This work was supported in part by a Grant-in-Aid (25461178) for Scientific Research (C) from the Japan Society for the Promotion of Science (http://www.jsps.go.jp/english/index.html), by a grant from the Ohyama Health Foundation (http://www.disclo-koeki.org/10a/01044/index.html) and by a Grant-in-Aid (H25-Shinko-Ippan-015) from the Ministry of Health, Labour, and Welfare, Japan (http://www.jsps.go.jp/english/e-grants/grants.html). The funders had no role in study design, data collection and analysis, decision to publish, or preparation of the manuscript.

Competing Interests: Yoshihiko Hoshino is a PLOS ONE Editorial Board member. This does not alter the authors' adherence to all PLOS ONE policies on sharing data and materials, as detailed online in the guide for authors.

Abstract

Mycobacterium abscessus group subsp., such as *M. massiliense, M. abscessus sensu stricto* and *M. bolletii*, are an environmental organism found in soil, water and other ecological niches, and have been isolated from respiratory tract infection, skin and soft tissue infection, postoperative infection of cosmetic surgery. To determine the unique genetic feature of *M. massiliense*, we sequenced the complete genome of *M. massiliense* type strain JCM 15300 (corresponding to CCUG 48898). Comparative genomic analysis was performed among *Mycobacterium* spp. and among *M. abscessus* group subspp., showing that additional ß-oxidation-related genes and, notably, the mammalian cell entry (*mce*) operon were located on a genomic island, *M. massiliense* Genomic Island 1 (MmGI-1), in *M. massiliense*. In addition, putative anaerobic respiration system-related genes and additional mycolic acid cyclopropane synthetase-related genes were found uniquely in *M. massiliense*. Japanese isolates of *M. massiliense* also frequently possess the MmGI-1 (14/44, approximately 32%) and three unique conserved regions (26/44; approximately 60%, 34/44; approximately 77% and 40/44; approximately 91%), as well as isolates of other countries (Malaysia, France, United Kingdom and United

States). The well-conserved genomic island MmGI-1 may play an important role in high growth potential with additional lipid metabolism, extra factors for survival in the environment or synthesis of complex membrane-associated lipids. ORFs on MmGI-1 showed similarities to ORFs of phylogenetically distant *M. avium* complex (MAC), suggesting that horizontal gene transfer or genetic recombination events might have occurred within MmGI-1 among *M. massiliense* and MAC.

Introduction

Nontuberculous mycobacteria (NTM) are classified into slowly growing mycobacterium (SGM) and rapidly growing mycobacterium (RGM) species; some of these bacteria cause pulmonary diseases [1]. Among RGM, the *Mycobacterium abscessus* group has been shown to be an emerging respiratory pathogen in cystic fibrosis, non-cystic-fibrosis bronchiectasis and chronic obstructive pulmonary disease [2, 3, 4, 5, 6], and is also an environmental organism found in soil, water and other ecological niches [7, 8]. The *M. abscessus* group consists of three subspecies, *M. abscessus* subsp. *abscessus* (*M. abscessus sensu stricto*), *M. abscessus* subsp. *massiliense* (*M. massiliense*) and *M. abscessus* subsp. *bolletii* (*M. bolletii*) [9, 10]. The three subspecies can generally be distinguished by phylogenetic analysis of the housekeeping gene, *rpoB*, and the macrolide resistance-related gene, erythromycin ribosome methyltransferase (*erm*) (41). Bryant *et al.* and Nakanaga *et al.* have recently reported more detailed classification methods, including, respectively, a whole-genome single nucleotide polymorphism (SNP) approach and a multiplex PCR method using insertion/deletion regions identified by whole-genome sequencing alignment analysis [4, 11]. Several subcutaneous infections following surgery, other medical treatments or traumatic injury have recently been found to be caused by *M. massiliense* [12, 13, 14, 15]. It was also recently reported that *M. massiliense* caused cutaneous infections that could not be attributed to a prior invasive procedure [16]. Phylogenetic analyses of the *M. abscessus* group have been performed, putative virulence factors of *M. abscessus sensu stricto* have been identified and studied, and the comparative whole-genome analysis of *M. abscessus* group isolated from patients of wide geographical origin have been performed [4, 17, 18, 19]; however, a detailed comparative analysis of *M. abscessus* group subspp. to determine *M. massiliense* unique genetic feature is lacking. Thus, in the current study, we sequenced the complete *M. massiliense* JCM 15300 (CCUG 48898) genome and compared it with that of *M. abscessus* group subspecies.

Results and Discussion

Genomic sequence of *M. massiliense* JCM 15300

The complete chromosomal sequence of *M. massiliense* JCM 15300 was obtained by *de novo* assembly of short reads followed by gap-closing using directed PCR. The genome consisted of 4,978,382 base pairs (bps) with a GC content of 64.1% and 4,950 predicted coding sequences (CDSs), 46 tRNA genes, one rRNA operon and two prophages (Fig. 1A). The chromosomal sequence corresponded to the predicted restriction fragment profiles obtained by PFGE analysis (data not shown). A draft genomic sequence of CCUG 48898 corresponding to JCM 15300 has been previously deposited in GenBank (NZ_AHAR01000000) by another research group. Thus, we performed a comparative pair-wise sequence alignment, revealing highly conserved synteny to the complete genomic sequence of JCM 15300 (S1 Figure and S1 Table). There were 188 mutations within 33 CDSs and 7 non-coding sites, suggesting that the differences between type strains may be due to frequent passaging and cultivation in various laboratories and bioresource centers. JCM15300 strain is smooth colony morphotype, and then there are no nonsense or frameshift mutations and in *mps1-mps2-gap* (MMASJCM_4183, MMASJCM_4184 and MMASJCM_4185) or *mmpl4b* (MMASJCM_4202) (data not shown), these data is consistent with a previous report [20].

Comparative genomic analysis within the *Mycobacterium* genus

To characterize the genomic features of *M. massiliense* JCM 15300, a BLAST atlas analysis was performed; corresponding orthologs in complete and draft genomic sequences of other *Mycobacterium* spp. were compared with those of *M. massiliense* JCM 15300 as a reference (*M. bolletii* BD is a draft genomic sequence, but it is closely related to *M. massiliense*) (Fig. 1A). The BLAST atlas identified the conserved proteins in the core genome, which was represented by 973 CDSs (19.7%) shared among all 15 *Mycobacterium* spp. genomes. *M. massiliense* JCM 15300 was highly similar to *M. abscessus* ATCC 19977 and *M. bolletii* BD in the *M. abscessus* group (Fig. 1B). In contrast, *M. massiliense* JCM 15300 showed a low similarity (~73% of mean identity) to SGM and other RGM (Fig. 1B). The 16S rRNA phylogenetic analysis suggested complete identity of *M. massiliense* JCM 15300 to *M. abscessus* ATCC 19977 and *M. bolletii* BD (Fig. 1C). These results indicate that *M. massiliense* is difficult to distinguish among the three *M. abscessus* subspecies using 16S rRNA gene phylogeny and that the three subspecies belong to the *M. abscessus* group as suggested by many reports.

The above analysis demonstrated that there were several highly variable gene clusters and notable differences in GC content (64.1%) among the 14 *Mycobacterium* spp. One prophage, located in the region from 1,816 to 1,880 kbs, had a lower GC content (59.64%) and partially shared some conserved CDSs with *M. abscessus* ATCC 19977 (gray bar in the lower right of Fig. 1A). The average GC content of all 14 *Mycobacterium* spp. and 620 mycobacteriophages [21] was approximately 66% and 64%, respectively, suggesting that the low-GC content

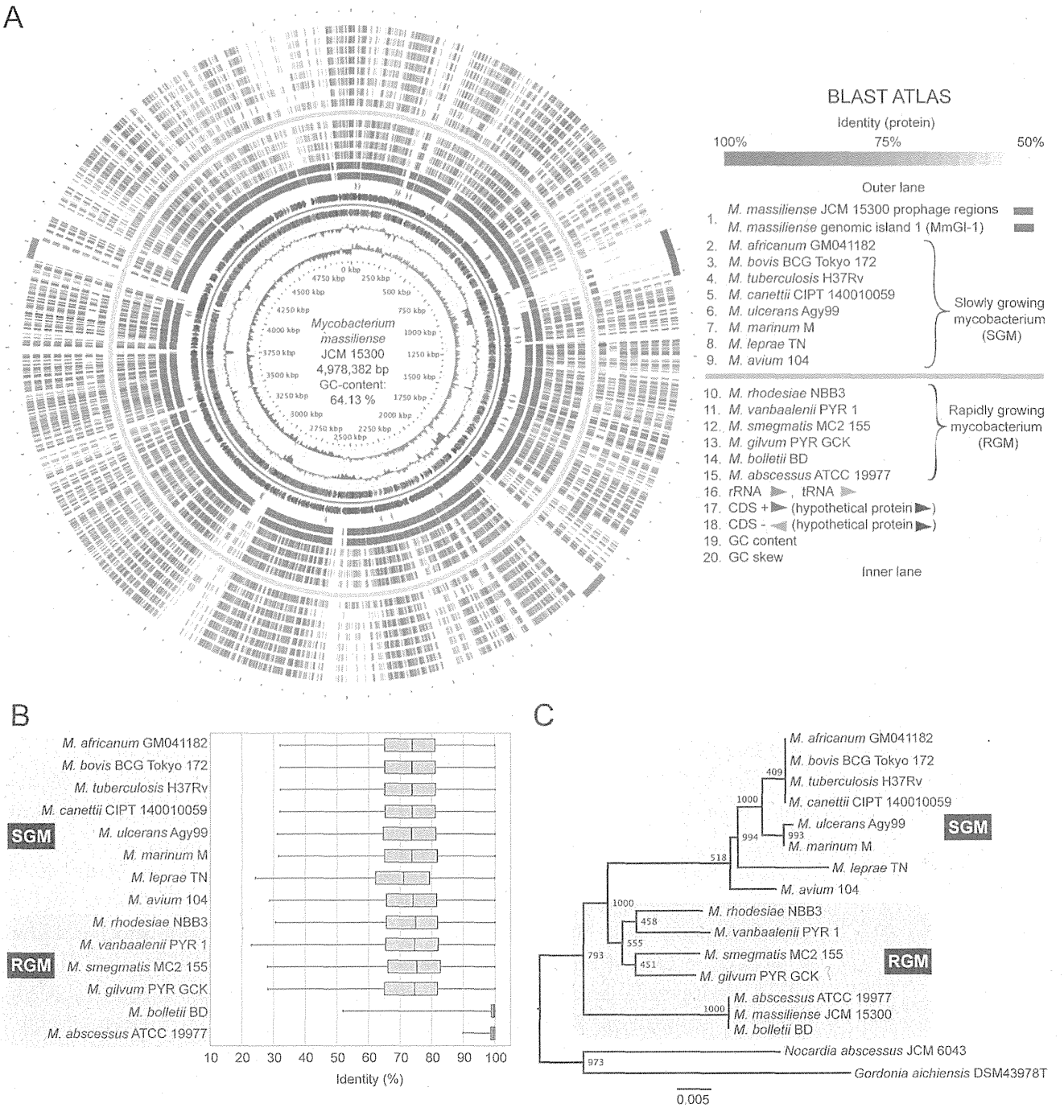

Fig. 1. Circular representation of the *M. massiliense* JCM 15300 genome and comparative analysis among the complete genomes of *Mycobacterium* species. A. BLAST atlas of *M. massiliense* JCM 15300. The coding region of strain JCM 15300 was aligned against those of 14 other *Mycobacterium* genomes using BLASTP. The results are displayed as colored circles with increasing color intensity signifying increased similarity. It was estimated that the number of conserved proteins was 1,516 among all 14 *Mycobacterium* genomes. B. Box plot of identity percentage of conserved proteins between *M. massiliense* JCM 15300 and 14 other *Mycobacterium* spp. The top of each box in the box plot indicates the 75th percentile, the bottom of each box indicates the 25th percentile and the center bar represents the median. C. Neighbor-joining phylogenetic tree based on 16S rRNA gene sequencing of *Mycobacterium* with 1,000-fold bootstrapping. Scale bar indicates number of substitutions per site. The number at each branch node represents the bootstrapping value. *Nocardia abscessus* JCM 6043 (GenBank: AF430018) and *Gordonia aichiensis* DSM43978T (X80633) were used as outgroups.

doi:10.1371/journal.pone.0114848.g001

prophage was recently acquired. In contrast, another prophage, located in the region from 3,964,186 to 4,013,302 bps, had an average GC content (64%), indicating that it could be specific to *M. massiliense* JCM 15300 (gray bar in the upper left of Fig. 1A).

Intriguingly, a notable genomic island from 946,561 to 1,057,603 bps, designated *M. massiliense* genomic island 1 (MmGI-1; indicated by the blue bar in the upper right of Fig. 1A), appeared to be conserved among *M. massiliense* JCM 15300, *M. bolletii* BD and *M. avium* 104. The genomic island contained gene clusters associated with lipid metabolism and lipid-related transporters (Fig. 2 and Table 1). ß-oxidation-related genes were also identified, such as long-chain fatty acid-CoA ligase (MMASJCM_1018, MMASJCM_1019, MMASJCM_1028), acyl-CoA dehydrogenase (MMASJCM_1023, MMASJCM_1030, MMASJCM_1035, MMASJCM_1038), enoyl-CoA hydratase (MMASJCM_1008, MMASJCM_1009, MMASJCM_1010, MMASJCM_1022), 3-hydroxyacyl-CoA dehydrogenase (MMASJCM_1006, MMASJCM_1034), acyl-CoA thiolase (MMASJCM_1016, MMASJCM_1036) and acetyl-CoA acetyltransferase (MMASJCM_1014) (Table 1).

An ortholog of the mammalian cell entry (*mce*) operon (MMASJCM_0985 to _0992) was found in the genomic island (Fig. 2 and Table 1). The *mce* operon of *Actinomycetales* species has been suggested to encode a subfamily of ATP-binding cassette (ABC) transporters that have a possible role in remodeling the cell envelope [22] and entry of the pathogen into non-phagocytic cells [23]. Although the function of the Mce protein family has not been clearly established, its members are believed to be membrane lipid transporters. For example, it has been demonstrated that the *mce4* operon is required for cholesterol utilization and uptake by *M. tuberculosis* [24] and *M. smegmatis* [25]. *M. massiliense* JCM 15300 contained 8 loci from the *mce* operon, and one *mce* operon on the MmGI-1 genomic island demonstrated approximately 99% similarity to that of *M. bolletii* BD and approximately 80% similarity to that of *M. avium* 104.

To characterize a provenance of MmGI-1 regions, the regions were subjected to BLASTN/BLASTP search against NCBI nt/nr databases excluding *M. abscesses* group sequences. Although the nucleotide search with BLASTN did not show notable homology to MmGI-1 region, the protein search with BLASTP showed that 105 ORFs on MmGI-1 showed significant similarity to ORFs of *Actinomycetales* with 32 to 95% identity. Of 105 ORFs, forty-two ORFs showed similarities to ORFs of phylogenetically distant *M. avium* complex (MAC) (Fig. 3), suggesting that the MmGI-1 region might have been acquired through horizontal gene transfer or genetic recombination events with MAC.

Using 55 draft genomic sequences from the *M. abscessus* group [17] and one complete genomic sequence from *M. massiliense* JCM 15300, variation among the genomic islands was investigated. The phylogeny of *M. abscessus* group strains was further characterized by identifying 203,267 SNPs in the commonly shared genomic sequence (Fig. 2). The SNP phylogenetic analysis identified three clusters (i.e., massiliense, bolletii and abscessus clusters) from the *M. abscessus* group, consistent with a previous report [17]. Phylogenetic and heatmap analyses

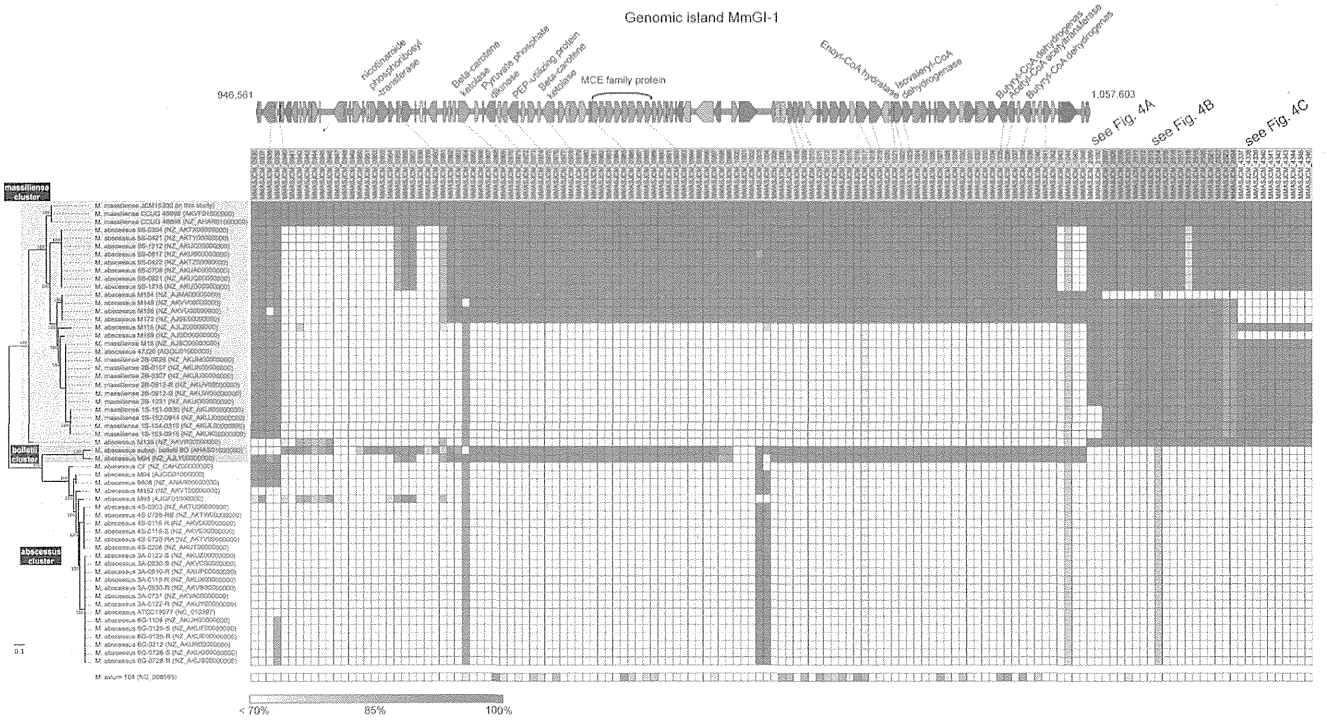

Fig. 2. Schematic representation of genomic island MmGI-1 and heatmap of MmGI-1, anaerobic respiration genes and mycolic acid synthase-related gene loci among 56 *M. abscessus* group strains. Phylogenetic tree based on 203,267 core genome SNPs in the whole-genome-sequenced *M. abscessus* group by the maximum-likelihood method with 1,000-fold bootstrapping. The scale indicates that a branch with a length of 0.1 is 10 times as long as one that would show a 1% difference between the nucleotide sequences at the beginning and end of the branch. The number at each branch node represents the bootstrapping value. The ORFs of *M. massiliense* strain JCM 15300 were aligned against the genomic sequences of 56 other *M. abscessus* group strains and *M. avium* 104 using TBLASTN (E-value cutoff, 1.00E-10; identity cutoff, 70%). A heatmap was constructed from amino acid identity.

doi:10.1371/journal.pone.0114848.g002

suggested that MmGI-1 was partially shared among *M. massiliense*-related strains (Fig. 2). Notably, the ß-oxidation-related loci (MMASJCM_0982 to _1042) were also well conserved in *M. bolletii* BD and M24. These additional lipid-related metabolic genes may be important for high growth potential with additional lipid metabolism such as putative ß-oxidation pathway, extra factors for survival in the environment (as suggested by the presence of MCE family protein) or synthesis of complex membrane-associated lipids (as suggested by the presence of a long-chain-fatty-acid-CoA ligase).

Comparative genomic analysis within the *M. abscessus* group

To characterize the genomes of the previously described three clusters, we performed further comparative and BLAST atlas analyses based on the nucleotide sequences of two complete genomes and the predicted amino acid sequences of CDSs, respectively (S2 Figure and S2 and S3 Table), and then also performed pan-genomic analysis with 30 *M. massiliense*, 2 *M, bolletii* and 25 *M. abscessus* genome sequences because of a validation (S3 Figure). The pan-genomic analysis data is consistent with a previous report [19]. The comparative analysis yielded

Table 1. Genes on the genomic island MmGI-1 *M. massiliense* JCM 15300.

Gene_ID	Location at JCM 15300	Strand	Length	Product	COG classifications*	KEGG orthology	BLASTP top hit seqeuence (E-value cutoff: 1E-1, database: nr without *M. abscessus* group data)			
							Accession number	Organisms	E-value	Identities
MMASJCM_0936	946561..947025	-	154	guanosine-3',5'-bis(Diphosphate) 3'-pyrophosphohydrolase	TK		WP_023955244.1	*Williamsia* sp. D3	7E-39	53.85%
MMASJCM_0937	947015..947167	-	50	hypothetical protein			WP_013871760.1	Frankia symbiont of Datisca glomerata	4E-06	47.73%
MMASJCM_0938	947284..949143	-	619	hypothetical protein	H		EUA75642.1	*M. chelonae* 1518	6E-161	69.98%
MMASJCM_0939	949143..949457	-	104	hypothetical protein	S		EUA75643.1	*M. chelonae* 1518	4E-22	54.74%
MMASJCM_0940	949859..950386	-	175	hypothetical protein			WP_015388818.1	*M. yongonense*	1E-72	66.27%
MMASJCM_0941	950404..951273	-	289	hypothetical protein	O		WP_023363492.1	*M. kansasii*	8E-67	49.62%
MMASJCM_0942	951280..952167	-	295	hypothetical protein	L		WP_023363490.1	*M. kansasii*	3E-118	62.93%
MMASJCM_0943	952344..952706	+	120	hypothetical protein	K		WP_015388820.1	*M. yongonense*	6E-37	68.42%
MMASJCM_0944	952851..953441	+	196	hypothetical protein			WP_015388821.1	*M. yongonense*	3E-54	61.96%
MMASJCM_0945	953484..954032	+	182	hypothetical protein			WP_015388822.1	*M. yongonense*	1E-69	58.56%
MMASJCM_0946	954019..955020	+	333	hypothetical protein			WP_015388823.1	*M. yongonense*	2E-154	72.50%
MMASJCM_0947	955027..955311	-	94	hypothetical protein	S		EWT07839.1	*Intrasporangium chromatiredu-cens* Q5-1	2E-34	64.89%
MMASJCM_0948	956934..958430	-	498	site-specific DNA-methyltransferase	L		WP_020097565.1	*Microbacterium* sp. 11MF	7E-177	63.77%
MMASJCM_0949	958473..958796	+	107	hypothetical protein			WP_011768395.1	*Mycobacterium* sp. KMS	3E-08	36.56%
MMASJCM_0950	958893..959312	-	139	hypothetical protein			WP_006339348.1	*Gordonia rhizosphera*	1E-14	31.85%
MMASJCM_0951	959512..960780	+	422	hypothetical protein			WP_029121465.1	*Mycobacterium* sp. UNC410CL29C-vi84	1E-165	58.18%
MMASJCM_0952	960806..961159	+	117	hypothetical protein			WP_020099065.1	*Mycobacterium*	5E-36	58.49%
MMASJCM_0953	961156..961461	-	101	hypothetical protein	S		WP_024801663.1	*Nocardia* sp. BMG51109	2E-09	35.42%
MMASJCM_0954	961458..961751	-	97	hypothetical protein	S		WP_020099063.1	*Mycobacterium*	2E-19	48.45%
MMASJCM_0955	961838..962734	+	298	phosphoribosylpyropho-sphate synthetase	FE		ETB46104.1	*M. avium* 10-5560	2E-48	51.56%
MMASJCM_0956	962749..964272	+	507	nicotinamide phosphori-bosyltransferase	H	K03462	ETB46369.1	*M. avium* 10-5560	0	71.69%

Table 1. Cont.

Gene_ID	Location at JCM 15300	Strand	Length	Product	COG classifications*	KEGG orthology	BLASTP top hit seqeuence (E-value cutoff: 1E-1, database: nr without *M. abscessus* group data)			
							Accession number	Organisms	E-value	Identities
MMASJCM_0957	964269..964919	+	216	possible DNA hydrolase	F	K03574	ETB46368.1	*M. avium* 10-5560	2E-66	53.00%
MMASJCM_0958	965195..965308	+	37	hypothetical protein			No hits found			
MMASJCM_0959	965479..965808	+	109	hypothetical protein	R		No hits found			
MMASJCM_0960	965980..967356	+	458	hypothetical protein	C		WP_024449466.1	*M. iranicum*	0	57.42%
MMASJCM_0961	967635..967844	-	69	hypothetical protein			WP_015388818.1	*M. yongonense*	9E-23	75.38%
MMASJCM_0962	968295..968783	-	162	hypothetical protein	S		WP_025089036.1	*Mycobacterium*	6E-47	50.00%
MMASJCM_0963	968949..969167	-	72	hypothetical protein			WP_015291571.1	*M. canettii*	5E-13	60.71%
MMASJCM_0964	969380..970636	-	418	putative cytochrome P450 IgrA	Q	K00517	EUA78264.1	*M. chelonae* 1518	0	88.04%
MMASJCM_0965	971395..971925	+	176	conserved hypothetical integral membrane protein YrbE1A	Q		WP_005143639.1	*M. rhodesiae*	1E-37	44.97%
MMASJCM_0966	971981..972526	-	181	transcriptional regulator, TetR family	K		WP_014384296.1	*M. intracellulare*	5E-53	50.00%
MMASJCM_0967	972591..973097	-	168	transcriptional regulator, TetR family	K		WP_014384297.1	*M. intracellulare*	2E-61	58.33%
MMASJCM_0968	973468..975162	+	564	beta-carotene ketolase	Q	K02292	CDO90343.1	*M. triplex*	0	91.41%
MMASJCM_0969	975672..976337	+	221	hypothetical protein	R		CDO30896.1	*M. vulneris*	5E-120	74.21%
MMASJCM_0970	976573..976902	+	109	hypothetical protein			WP_010228994.1	*Pseudonocardia* sp. P1	5E-27	52.88%
MMASJCM_0971	976927..978438	-	503	pyruvate, phosphate dikinase	G	K01006	WP_011726421.1	*M. avium*	0	72.06%
MMASJCM_0972	978435..979052	-	205	hypothetical protein	K		KDO99916.1	*M. avium* subsp. *hominissuis* 101	1E-95	67.80%
MMASJCM_0973	979096..980010	-	304	hypothetical protein			WP_011726419.1	*M. avium*	2E-177	79.28%
MMASJCM_0974	980007..981524	-	505	hypothetical protein	G	K01007	KBR61967.1	*M. tuberculosis* XTB13-223	0	73.76%
MMASJCM_0975	981770..982378	+	202	transcriptional regulator, TetR family	K		WP_011726417.1	*M. avium*	1E-85	66.67%
MMASJCM_0976	982618..983658	+	346	hypothetical protein			CDO30900.1	*M. vulneris*	0	87.32%
MMASJCM_0977	983932..984459	+	175	transcriptional regulator, TetR family	K		CDO90192.1	*M. triplex*	2E-61	60.00%
MMASJCM_0978	984571..986193	-	540	beta-carotene ketolase	Q		KDE98300.1	*M. aromaticivorans* JS19b1	0	82.45%
MMASJCM_0979	986685..987560	+	291	hypothetical protein			KDE98305.1	*M. aromaticivorans* JS19b1	2E-175	83.74%
MMASJCM_0980	987577..988209	-	210	transcriptional regulator, TetR family	K		KDE98304.1	*M. aromaticivorans* JS19b1	1E-95	76.60%

Table 1. Cont.

Gene_ID	Location at JCM 15300	Strand	Length	Product	COG classifications*	KEGG orthology	BLASTP top hit seqeuence (E-value cutoff: 1E-1, database: nr without *M. abscessus* group data)			
							Accession number	Organisms	E-value	Identities
MMASJCM_0981	988316..989380	+	354	hypothetical protein			KDE98303.1	*M. aromaticivorans* JS19b1	0	77.68%
MMASJCM_0982	989396..990508	+	370	putative phosphotransferase	R		WP_005141265.1	*M. rhodesiae*	0	75.41%
MMASJCM_0983	990691..990807	+	38	hypothetical protein			No hits found			
MMASJCM_0984	990970..991083	-	37	hypothetical protein			No hits found			
MMASJCM_0985	991197..992228	+	343	putative YrbE family protein	Q		KBR61969.1	*M. tuberculosis* XTB13-223	2E-148	88.21%
MMASJCM_0986	992228..993097	+	289	putative Mce family protein	Q		KBR61970.1	*M. tuberculosis* XTB13-223	8E-168	80.28%
MMASJCM_0987	993105..994199	+	364	putative Mce family protein	Q		CDO30921.1	*M. vulneris*	0	70.56%
MMASJCM_0988	994196..995203	+	335	putative Mce family protein	Q		WP_011726414.1	*M. avium*	0	75.52%
MMASJCM_0989	995221..996162	+	313	putative Mce family protein	Q		KBR61973.1	*M. tuberculosis* XTB13-223	1E-176	77.96%
MMASJCM_0990	996132..997280	+	382	putative Mce family protein	Q		KDO99908.1	*M. avium* subsp. *hominissuis* 101	0	67.28%
MMASJCM_0991	997277..998266	+	329	putative Mce family protein	Q		WP_024637000.1	*M. avium*	2E-162	69.39%
MMASJCM_0992	998263..999219	+	318	putative Mce family protein	Q		CDO30926.1	*M. vulneris*	3E-157	69.50%
MMASJCM_0993	999262..999906	+	214	hypothetical protein			WP_007170571.1	*M. parascrofulaceum*	1E-82	61.27%
MMASJCM_0994	999982..1000584	+	200	hypothetical protein			KDE98251.1	*M. aromaticivorans* JS19b1	5E-88	65.83%
MMASJCM_0995	1000670..1001113	+	147	hypothetical protein			CDO30929.1	*M. vulneris*	7E-48	63.20%
MMASJCM_0996	1001158..1001496	+	112	hypothetical protein			WP_007170568.1	*M. parascrofulaceum*	4E-44	62.39%
MMASJCM_0997	1001544..1002104	+	186	hypothetical protein			CDO30931.1	*M. vulneris*	5E-91	75.71%
MMASJCM_0998	1002279..1002410	+	43	hypothetical protein			No hits found			
MMASJCM_0999	1002407..1003372	-	321	hypothetical protein	O		WP_014711294.1	*Mycobacterium* sp. MOTT36Y	0	80.94%
MMASJCM_1000	1003379..1004497	-	372	putative phosphotransferase	R		CDO90200.1	*M. triplex*	0	68.01%
MMASJCM_1001	1004938..1007496	-	852	hypothetical protein	K		WP_030203671.1	*Pilimelia anulata*	0	72.98%

Table 1. Cont.

Gene_ID	Location at JCM 15300	Strand	Length	Product	COG classifications*	KEGG orthology	BLASTP top hit seqeuence (E-value cutoff: 1E-1, database: nr without *M. abscessus* group data)			
							Accession number	Organisms	E-value	Identities
MMASJCM_1002	1007489..1008-457	-	322	cell division protein FtsH	O		WP_022566726.1	*Nocardia asteroides*	0	88.51%
MMASJCM_1003	1009865..1010-737	+	290	hypothetical protein			EUA78068.1	*M. chelonae* 1518	4E-180	95.32%
MMASJCM_1004	1010796..1013-315	+	839	hypothetical protein	D		WP_005113273.1	*M. chelonae*	0	94.89%
MMASJCM_1005	1015076..1015-558	-	160	hypothetical protein	Q		WP_013873946.1	Frankia symbiont of Datisca glomerata	3E-23	45.45%
MMASJCM_1006	1015591..1016-388	-	265	2-hydroxycyclohexane-carboxyl-CoA dehydrogenase	IQR		WP_011726451.1	*M. avium*	1E-162	83.77%
MMASJCM_1007	1016500..1017-249	+	249	3-oxoacyl-[acyl-carrier protein] reductase	IQR	K00059	WP_023985895.1	*M. neoaurum*	2E-135	80.82%
MMASJCM_1008	1017246..1018-016	+	256	enoyl-CoA hydratase	I	K15866	WP_011726449.1	*M. avium*	8E-104	66.54%
MMASJCM_1009	1018013..1018-810	+	265	enoyl-CoA hydratase	I	K15866	WP_011726448.1	*M. avium*	4E-145	82.95%
MMASJCM_1010	1018810..1019-595	+	261	enoyl-CoA hydratase	I	K15866	WP_029114372.1	*Mycobacterium* sp. URHB0044	7E-120	70.93%
MMASJCM_1011	1019592..1020-860	+	422	putative dioxygenase hydroxylase component	PR	K05549	WP_030136631.1	*M. neoaurum*	0	86.46%
MMASJCM_1012	1021187..1021-393	+	68	beta subunit of hydroxylase component of benzoate 1,2-dioxygenase	Q		WP_011726445.1	*M. avium*	3E-26	77.05%
MMASJCM_1013	1021459..1021-659	+	66	hypothetical protein	T		WP_030136633.1	*M. neoaurum*	3E-29	81.54%
MMASJCM_1014	1021938..1022-864	+	308	acetyl-CoA acetyltransferase	I	K00626	WP_014384231.1	*M. intracellulare*	0	84.36%
MMASJCM_1015	1022861..1024-216	+	451	hydroxymethylglutaryl-CoA synthase	I		WP_011726442.1	*M. avium*	0	73.38%
MMASJCM_1016	1024206..1025-411	+	401	putative thiolase	I		WP_011726441.1	*M. avium*	0	88.35%
MMASJCM_1017	1025490..1026-350	+	286	probable short-chain type dehydrogenase reductase	IQR	K12405	WP_011726440.1	*M. avium*	4E-172	84.27%
MMASJCM_1018	1026409..1028-046	+	545	long-chain-fatty-acid—CoA ligase	IQ	K01911	WP_011726439.1	*M. avium*	0	66.42%
MMASJCM_1019	1028043..1029-800	+	585	long-chain-fatty-acid—CoA ligase	IQ		WP_011726438.1	*M. avium*	0	68.67%

Table 1. Cont.

Gene_ID	Location at JCM 15300	Strand	Length	Product	COG classifications*	KEGG orthology	BLASTP top hit seqeuence (E-value cutoff: 1E-1, database: nr without *M. abscessus* group data)			
							Accession number	Organisms	E-value	Identities
MMASJCM_1020	1029761..1030-786	-	341	hypothetical protein	R		WP_023985889.1	*M. neoaurum*	7E-128	57.19%
MMASJCM_1021	1030966..1031-418	+	150	acyl dehydratase	I		WP_003923910.1	*M. thermoresis-tibile*	2E-76	75.00%
MMASJCM_1022	1031408..1032-619	+	403	enoyl-CoA hydratase	I	K15866	WP_007170622.1	*M. parascrofulaceum*	2E-174	67.74%
MMASJCM_1023	1032620..1033-783	+	387	isovaleryl-CoA dehydrogenase	I		WP_007170621.1	*M. parascrofulaceum*	0	81.61%
MMASJCM_1024	1033815..1035-116	+	433	phytoene dehydrogenase family protein	Q		WP_007170620.1	*M. parascrofulaceum*	0	81.73%
MMASJCM_1025	1035104..1035-961	+	285	citrate lyase beta chain	G	K01644	WP_007170619.1	*M. parascrofulaceum*	9E-111	66.92%
MMASJCM_1026	1036061..1036-291	-	76	hypothetical protein			No hits found			
MMASJCM_1027	1036800..1037-204	+	134	hypothetical protein	I		CDO90349.1	*M. triplex*	4E-79	88.06%
MMASJCM_1028	1037208..1038-746	+	512	long-chain-fatty-acid—CoA ligase	IQ	K00666	WP_030136653.1	*M. neoaurum*	0	76.32%
MMASJCM_1029	1038743..1040-002	+	419	putative cytochrome P450 hydroxylase	Q	K00517	CDO30946.1	*M. vulneris*	0	90.31%
MMASJCM_1030	1040014..1040-805	+	263	3-alpha-hydroxysteroid dehydrogenase	IQR		WP_019509868.1	*M. neoaurum*	9E-156	82.89%
MMASJCM_1031	1040815..1042-215	+	466	aldehyde dehydrogenase	C	K00128	WP_003923898.1	*M. thermoresis-tibile*	0	75.28%
MMASJCM_1032	1042215..1042-406	+	63	hypothetical protein	C		WP_005141491.1	*M. rhodesiae*	3E-19	66.13%
MMASJCM_1033	1042569..1044-056	+	495	ferredoxin—NADP(+) reductase	ER	K00528	KBR61952.1	*M. tuberculosis* XTB13-223	0	64.02%
MMASJCM_1034	1044016..1045-248	+	410	4-hydroxybutyrate coenzyme A transferase	C		WP_011726433.1	*M. avium*	0	69.07%
MMASJCM_1035	1045317..1046-471	-	384	butyryl-CoA dehydrogenase	I		WP_019509874.1	*M. neoaurum*	0	84.03%
MMASJCM_1036	1046475..1047-626	-	383	acetyl-CoA acetyltransferase	I	K07823	WP_011726431.1	*M. avium*	0	87.21%
MMASJCM_1037	1047688..1048-263	-	191	transcriptional regulator, TetR family	K		WP_030136662.1	*M. neoaurum*	6E-93	71.96%
MMASJCM_1038	1048446..1049-600	-	384	butyryl-CoA dehydrogenase	I	K00248	WP_014941082.1	*M. indicus pranii*	0	84.38%
MMASJCM_1039	1049725..1050-264	-	179	transcriptional regulator, TetR family	K		WP_019509888.1	*M. neoaurum*	3E-67	60.12%

Table 1. Cont.

Gene_ID	Location at JCM 15300	Strand	Length	Product	COG classifications*	KEGG orthology	BLASTP top hit seqeuence (E-value cutoff: 1E-1, database: nr without *M. abscessus* group data)			
							Accession number	Organisms	E-value	Identities
MMASJCM_1040	1050416..1051-048	-	210	transcriptional regulator, TetR family	K		WP_005146732.1	*M. rhodesiae*	6E-102	74.00%
MMASJCM_1041	1051285..1052-259	+	324	hypothetical protein	I		WP_003938179.1	*Rhodococcus ruber*	5E-121	60.67%
MMASJCM_1042	1052411..1053-019	+	202	transcriptional regulator, TetR family protein, putative	K		WP_014384219.1	*M. intracellulare*	5E-97	71.14%
MMASJCM_1043	1053327..1053-584	+	85	hypothetical protein			WP_005111625.1	*M. chelonae*	2E-21	58.54%
MMASJCM_1044	1053701..1055-929	+	742	carbonic anhydrase	P	K01673	WP_005057131.1	*M. chelonae*	0	76.16%
MMASJCM_1045	1056430..1056-960	+	176	hypothetical protein			WP_028655880.1	*Nocardioides* sp. J54	2E-11	32.62%
MMASJCM_1046	1057007..1057-603	+	198	hypothetical protein	G		WP_003960345.1	*Streptomyces clavuligerus*	2E-05	37.18%

*COG codes is as follows: C: Energy production and conversion, D: Cell cycle control, cell division, chromosome partitioning, E: Amino acid transport and metabolism, F: Nucleotide transport and metabolism, G: Carbohydrate transport and metabolism, H: Coenzyme transport and metabolism, I: Lipid transport and metabolism, K: Transcription, L: Replication, recombination and repair, O: Posttranslational modification, protein turnover, chaperones, P: Inorganic ion transport and metabolism, Q: Secondary metabolites biosynthesis, transport and catabolism, R: General function prediction only, S: Function unknown, T: Signal transduction mechanisms.

doi:10.1371/journal.pone.0114848.t001

the following four results: i) as a massiliense cluster-specific feature, there were six unique regions (†[1–6] in S2 Figure and Table 2) that contained an average GC content of 64%; ii) as a JCM 15300-specific feature, there were 10 unique regions (• in S2 Figure and S2 Table) that had relatively low GC content; iii) the MmGI-1 genomic island (Fig. 3 and ¶ in S2 Figure) was shared with *M. bolletii* and showed partial similarity to *M. avium* 104; iv) there were two common deletions (†[7–8] in S2 Figure and S3 Table) in the massiliense cluster and one conserved region in the abscessus group (§ in S2 Figure and S3 Table).

In addition to the MmGI-1 genomic island described above, the massiliense cluster contained three notable conserved loci: i) a molybdopterin oxidoreductase (Fig. 2, Fig. 4A and Table 2); ii) universal stress proteins, an alcohol dehydrogenase and a xylulose-5-phosphate phosphoketolase (Fig. 2, Fig. 4B and Table 2); iii) a cyclopropane fatty acyl-phospholipid synthase and an S-adenosyl-L-methionine-dependent methyltransferase (Fig. 2, Fig. 4C and Table 2). In contrast to MmGI-1, these three regions were well conserved within the massiliense cluster.

Choo *et al.* previously reported that a high proportion of accessory strain-specific genes indicating an open, non-conservative pan-genome structure, and clear evidence of rapid phage-mediated evolution [19]. In fact, specific genes in *M. massiliense* JCM15300 contained phage-related genes, i.e. putative prophage integrase (S2 Table). On the other hand, in adjacent gene loci of three conserved regions, i.e. MMASJCM-2099..2100, MMASJCM-2507..2524 and MMASJCM-4337..4346, there are no phage-related genes (Fig. 4 and Table 2). These data suggest that these conserved regions might be core-genome regions in ancestral *M. abscessus* group, and then have been deleted from genomes of *M. abscessus* and *M. bolletii.*

Prevalence of MmGI-1 and massiliense cluster unique regions in Japanese *M. massiliense* and *M. abscessus* isolates

We examined the prevalence of MmGI-1 and three massiliense cluster unique regions in Japanese *M. massiliense* and *M. abscessus* isolates using conventional PCR methods (S4 Table), because of *in silico* analysis using only isolates of Malaysia, France, United Kingdom and United States. The ratio of MmGI-1 positive *M. massiliense* and *M. abscessus* was 31.8% (14/44) and 1.4% (1/70), respectively (Fig. 5A and S5 Table). Applying Fisher's exact test, the proportion of MmGI-1 positive *M. massiliense* is significantly higher than that of *M. abscessus* (P=0.0001). *M. massiliense* frequently possesses three massiliense cluster unique regions in not only Japanese but also other countries (Malaysia, France and United States) isolates (Fig. 5A and S5 Table), suggesting that MmGI-1 and the massiliense cluster unique regions are highly conserved in *M. massiliense* isolated from various countries.

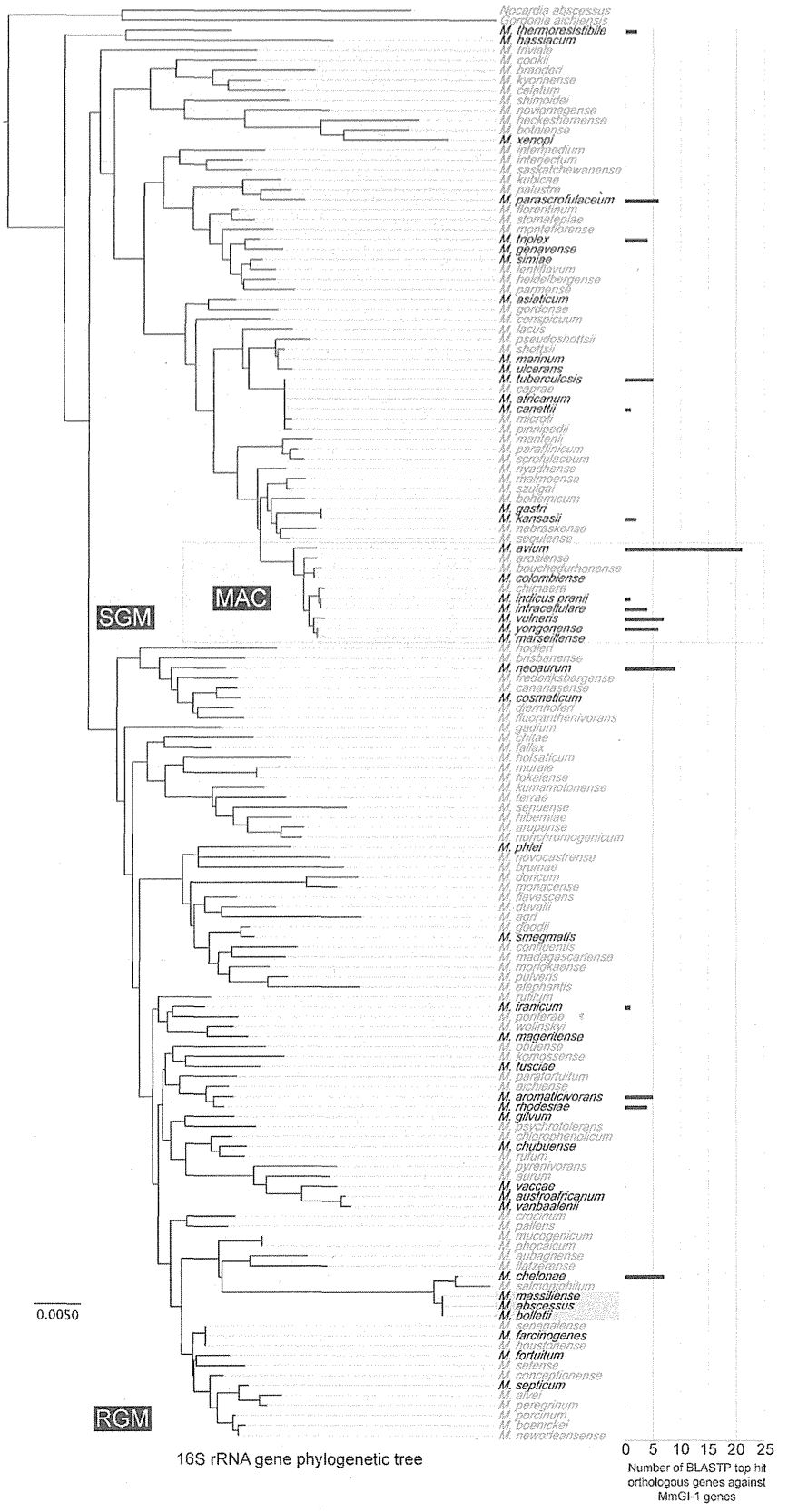

16S rRNA gene phylogenetic tree

Fig. 3. Orthologous genes of MmGI-1 genes in *Mycobacterium* spp. without *M. abscessus* group. Phylogenetic tree based on the 16S rRNA was constructed by Neighbor-joining method with 1,000-fold bootstrapping. Scale bar indicates number of substitutions per site. Species of black characters indicate that complete or draft genome sequences have been deposited at DDBJ/EMBL/GenBank. *M. abscessus* group is labeled by a yellow box. The number of BLASTP top hit orthologous genes against MmGI-1 genes are shown with a right bar chart.

doi:10.1371/journal.pone.0114848.g003

Growth ability of MmGI-1 positive *M. massiliense*

The massiliense cluster contained a conserved molybdopterin oxidoreductase as described above, and an ortholog was also identified in the strictly anaerobic bacterium, *Desulfitobacterium hafniense*. It has been reported that molybdopterin oxidoreductase may provide the ability for anaerobic energy metabolism [26]. The xylulose-5-phosphate phosphoketolase may play a role in heterolactic fermentation in anaerobic heterolactic acid bacteria, including *Lactobacillus* and *Leuconostoc* organisms [27]. Moreover, the universal stress protein in *Pseudomonas aeruginosa* has been reported to have a crucial role in survival under anaerobic conditions [28]. These studies suggest that *M. massiliense* may grow or survive under anaerobic or hypoxic conditions. Indeed, the oxygen partial pressure in various tissues is approximately 20–50 mm Hg (3–7% oxygen) [29, 30, 31, 32]. To determine growth ability under hypoxic conditions, 27 smooth colony morphology isolates (12 *M. abscessus*, 8 MmGI-1 positive *M. massiliense* and 7 MmGI-1 negative *M. massiliense* isolates) were subjected to aerobic and microaerobic (approximately 6% O_2) conditions (Fig. 5B and 5C), because the aggregation of rough colony morphology isolates were hard to measure the degree of turbidity in the broth culture. In aerobic condition, MmGI-1 positive *M. massiliense* isolates show well growth than MmGI-1 negative isolates including *M. abscessus* (Fig. 5B). On the other hand, in microaerobic condition, the growth didn't show significant differences between *M. massiliense* and *M. abscessus* (Fig. 5C). MMASJCM-2099..2100 and MMASJCM-2057..2524 regions highly conserved in *M. massiliense* isolated from Japan, Malaysia, France, United Kingdom and United States, as well as MmGI-1. Although functions of these regions are still unclear, the importance of MmGI-1 might be supported by the existence on these conserved regions in *M. massiliense*, and MmGI-1 might relate to high growth potential with additional lipid metabolism such as putative ß-oxidation pathway.

Phylogenetic analysis of mycolic acid synthase-related genes

The comparative genomic analysis indicated that *M. massiliense* including Japanese isolates possessed two extra CDSs that are possibly involved in the cyclopropanation of mycolic acid. A cyclopropane fatty acyl-phospholipid synthase (MMASJCM_4340) and an S-adenosyl-L-methionine-dependent methyltransferase (MMASJCM_4343) were detected only in the massiliense cluster (Fig. 4C). Both putative proteins encoded by these CDSs possessed the mycolic acid cyclopropane synthetase (CMAS) domain (pfam02353).

Table 2. The unique conserved gene loci in massiliense cluster among *M. abscessus* group.

Gene_ID	Location at JCM 15300	Strand	Length	Product	Note
MMASJCM_0834	825792..826802	-	336	transcriptional regulator	
MMASJCM_0835	826913..827713	+	266	short chain dehydrogenase	
MMASJCM_2099	2098058..2101435	-	1125	putative molybdopterin oxidoreductase	see Fig. 4A
MMASJCM_2100	2101513..2102112	+	199	putative transcriptional regulator	see Fig. 4A
MMASJCM_2410	2427416..2427601	-	61	hypothetical protein	
MMASJCM_2411	2427632..2428042	+	136	hypothetical protein	
MMASJCM_2412	2428054..2428788	+	244	hypothetical protein	
MMASJCM_2507	2509971..2510735	-	254	universal stress protein family	see Fig. 4B
MMASJCM_2508	2510875..2511216	-	113	universal stress protein family	see Fig. 4B
MMASJCM_2509	2511996..2512505	+	169	probable conserved transmembrane protein	see Fig. 4B
MMASJCM_2510	2512542..2513558	+	338	alcohol dehydrogenase	see Fig. 4B
MMASJCM_2511	2513572..2514579	-	335	hypothetical protein	see Fig. 4B
MMASJCM_2512	2514754..2515698	+	314	universal stress protein family	see Fig. 4B
MMASJCM_2513	2515695..2518106	+	803	xylulose-5-phosphate phosphoketolase	see Fig. 4B
MMASJCM_2514	2518103..2518852	+	249	two component transcriptional regulatory protein DevR	see Fig. 4B
MMASJCM_2515	2518819..2519823	+	334	sensor kinase	see Fig. 4B
MMASJCM_2516	2519946..2520536	+	196	histidine kinase response regulator	see Fig. 4B
MMASJCM_2517	2520544..2521497	+	317	sulfate transporter	see Fig. 4B
MMASJCM_2518	2521466..2522251	+	261	sulfate transporter	see Fig. 4B
MMASJCM_2519	2522241..2522855	-	204	hypothetical protein	see Fig. 4B
MMASJCM_2520	2522957..2523163	-	68	hypothetical protein	see Fig. 4B
MMASJCM_2521	2523183..2524058	-	291	universal stress protein family	see Fig. 4B
MMASJCM_2522	2524296..2525168	+	290	universal stress protein family	see Fig. 4B
MMASJCM_2523	2525188..2525475	+	95	hypothetical protein	see Fig. 4B
MMASJCM_2524	2525508..2525942	+	144	hypothetical protein	see Fig. 4B
MMASJCM_2869	2886124..2887602	+	492	carotenoid oxygenase	
MMASJCM_2870	2887612..2888793	+	393	two-component system	
MMASJCM_2871	2888790..2889410	+	206	two component transcriptional regulator	
MMASJCM_2872	2890468..2892372	-	634	hypothetical protein	
MMASJCM_2989	3016494..3018116	+	540	diaminopimelate decarboxylase	
MMASJCM_3589	3593912..3594541	-	209	transcriptional regulator	
MMASJCM_3590	3594814..3595809	+	331	2-amino-3-carboxymuconate-6-semialdehyde decarboxy-lase	
MMASJCM_4337	4335727..4337094	-	455	deoxyribodipyrimidine photolyase	see Fig. 4C
MMASJCM_4338	4337091..4338449	-	452	cell division inhibitor	see Fig. 4C
MMASJCM_4339	4338477..4339142	-	221	hypothetical protein	see Fig. 4C
MMASJCM_4340	4339165..4340058	-	297	cyclopropane-fatty-acyl-phospholipid synthase	see Fig. 4C
MMASJCM_4341	4340280..4341596	+	438	amine oxidase	see Fig. 4C
MMASJCM_4342	4341593..4342330	+	245	hypothetical protein	see Fig. 4C
MMASJCM_4343	4342327..4343601	+	424	S-adenosyl-L-methionine dependent methyltransferase	see Fig. 4C
MMASJCM_4344	4343598..4344383	+	261	hypothetical protein	see Fig. 4C
MMASJCM_4345	4344416..4344961	+	181	RNA polymerase sigma-70 factor	see Fig. 4C
MMASJCM_4346	4344943..4345665	+	240	hypothetical protein	see Fig. 4C

doi:10.1371/journal.pone.0114848.t002

Mycobacterium spp. possess 3 to 10 paralogs with a CMAS domain; for example, CmaA (cyclopropane mycolic acid synthase) and MmaA (methyl mycolic acid synthase) have been well characterized [33]. A phylogenetic analysis of CMAS domain-related proteins has indicated that one of the two extra proteins, MMASJCM_4340, is orthologous to MSMEG_1351 of *M. smegmatis* and MycrhN_0769/MycrhN_3064 of *M. rhodesiae* (S4 Figure). The other protein, MMASJCM_4343, is orthologous to UfaA1 (cyclopropane fatty acid synthase), which is present in a part of RGM and SGM species. The function of UfaA1 in mycolate biosynthesis is not clear [34]. The massiliense cluster has two unique mycolic acid synthesis-associated proteins that are not present in the abscessus or bolletii clusters.

Conclusions

The *M. abscessus* group is classified as RGM species and consists of three closely related organisms, *M. abscessus, M. bolletii* and *M. massiliense.* A comparative analysis based on three clusters in the *M. abscessus* group revealed that a genomic island MmGI-1 of *M. massiliense* may be involved in high growth potential with additional lipid metabolism such as putative ß-oxidation pathway. Moreover, MmGI-1 is conserved in *Actinomycetales*, especially *Mycobacterium*, and horizontal gene transfer or genetic recombination events might have occurred within MmGI-1 among *M. massiliense* and MAC. Although *M. abscessus* subspp. is an environmental organism found in soil, water and other ecological niches, the difference of detail ecological niches is still unclear among subspecies-level. Our data suggests that the massiliense cluster unique regions including MmGI-1 might be linked to differences in ecological niches, such as lipid rich environment, of *M. massiliense* and *M. abscessus.* Further studies are required to understand the specific genetic features identified in this study.

Materials and Methods

Bacterial strains

We sequenced *Mycobacterium massiliense* type strain JCM 15300 (CCUG 48898), which was originally isolated from the sputum of a 50-year-old woman with an 8-year history of bronchiectasis and hemoptysis [35]. This strain was obtained from the Japan Collection of Microorganisms at the Riken BioResource Center (BRC-JCM; Saitama, Japan) on September 18, 2009.

Short-read DNA sequencing

An *M. massiliense* strain DNA library (insert size of ~600 bp) was prepared using the Nextera DNA Sample Prep Kit (Illumina-compatible) (EPICENTRE Biotechnologies, Madison, WI). DNA clusters were generated on a slide using the Cluster Generation Kit (ver. 4) on an Illumina Cluster Station (Illumina, San